Using a Quantum Driven Adiabatic Free Energy Dynamics Computation to Uncover the Effects of Cage Flexibility on the Diffusion of Hydrogen Between Two Clathrate Cages

Philip Daniel Brous

ABSTRACT

Alternative energy research is turning towards hydrogen as a means of storing renewable energy sources, such as solar energy, and of providing clean fuel to motor vehicles. Storing the gas itself, however, proves to be a difficult task due to the small size of the atoms and low density of the gas. Scientists have expressed interest in clathrate hydrates, crystal lattices of cages made of water molecules, in the past twenty years for their potential to solve the issues of hydrogen storage. The goal is to eventually create a marketable product, but before this can be done, accurate data on clathrate hydrates must be obtained in order to prove their value. Until the cage-to-cage diffusion mechanism of hydrogen gas within the crystal lattice is fully understood, such data cannot be obtained. The flexibility of the clathrate cages has been theorized to play a role in diffusion, but this has yet to be verified numerically. This study seeks to answer this problem and provide some direction for the future of clathrate research. Using the theory of driven adiabatic free energy dynamics, programs were written to obtain the free energy profile for diffusion at several temperatures, assuming rigid cages. Using quantum transition state theory, rates were also obtained. Observation of the differences between the results of this study and a prior study, which obtained the same results but with flexible cages, led to the conclusion that flexibility does indeed play a role in diffusion. This indicates that scientists must take into account flexibility as a factor in future simulations.

INTRODUCTION

Background
1) Use of Hydrogen: Alternative Energy researchers want to use hydrogen as a means of storing renewable energy sources → renewable energy economy
2) Problems with Hydrogen Storage: Hydrogen storage is difficult since conditions to maintain it in a dense form demand a large amount on money and energy
3) Benefits of Clathrate Hydrates: Clathrate hydrates could solve these problems since it's energy dense, stable at higher temperatures, and made of water, one of the cheapest resources
4) Barriers to Clathrate Hydrate Technology: To market this product, accurate data about how well it retains hydrogen is a necessity
5) Current Research: Through simulation, scientists want to understand the processes involved in diffusion, which will help them calculate data when they scale up simulations

Literature Review
Early studies found initial data on clathrate hydrates, but most of it was not yet sufficiently accurate and also only scratched the surface (ref. 25, 31).
- An early study found the physical size of clathrate cages and initial cage occupation data experimentally (ref. 25). It provided accurate enough experimental data to use as simulation inputs, such as cage size, but it didn't find solid enough data on cage occupation numbers.
- Another study in 2005 followed up (ref. 31), finding that the small cages are singly occupied, but had yet to go any deeper.

Migration rates were further investigated with more intricate experimental and theoretical studies, but they still had limitations (ref. 32, 33).
- A slightly later study found data on migration rates at different temperatures (ref. 32), but the model was too basic for sufficiently accurate data, so more work needed to be done.
- Another experimental study provided slightly more accurate cage-to-cage migration data (ref. 33), but this was still too inaccurate, as it only examined ortho-hydrogen, and not para-hydrogen, meaning that at certain temperatures, only a small percentage of hydrogen present was investigated.

Later studies provided more insight into clathrate hydrates, including detailed analysis of migration rates and inclusion of quantum effects. But up to this point, no study has investigated the problem with regards to cage flexibility (ref. 30, 27).
- A 2015 study used a more advanced model to investigate both large-to-small cage and large-to-large cage diffusion (ref. 30). This study, however, failed to account for quantum effects.
- This proved to be a problem when a 2016 study investigated diffusion under a quantum system and concluded that quantum effects play a significant role around lower temperatures (ref. 27).
- However, a question that remained unanswered in all of these studies was whether or not flexibility plays a role. This study answers that question.

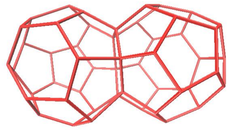

Figure 1. Visualization of a sII* clathrate hydrate, specifically two of the large cages connected at a hexagonal face. Hydrogen atoms have been omitted for clarity, and lines between oxygen atoms have been drawn to illustrate the cage structure (created using VMD).

Research Problem
Flexibility is an issue that has yet to be addressed but could have a large effect on the results.

Hypothesis
If the free energy surface for cage-to-cage diffusion for hydrogen in the sII* clathrate hydrate is obtained while assuming rigidity of the cages, then the data will be significantly different from that obtained by taking into account the flexibility of the cages.

*sII is a specific lattice structure for clathrate hydrates, and is thought to have the most potential out of any clathrate structure for efficient hydrogen storage.

Significance
Once the issue of flexibility is resolved, diffusion data at the small scale will be closer if not at the point where simulation can be scaled up

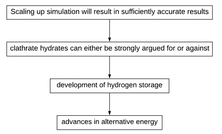

Figure 2. Flowchart explaining the significance.

METHODS

Path Integral Molecular Dynamics

- Feynman's path integral formulation → particles act like necklaces made of springs and beads
- Centroid is commonly taken before quantities such as free energy are calculated → efficiency (yet in some cases leads to inaccuracy)

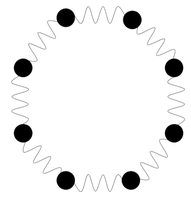

Figure 3. Bead-spring model of an atom.

$$Q_P(N,V,T) = \prod_{i=1}^{N}\left(\frac{m_i P}{2\pi\beta\hbar^2}\right)^{dP/2}\int\prod_{i=1}^{N}\mathrm{d}\mathbf{r}_i^{(1)}\cdots\mathrm{d}\mathbf{r}_i^{(P)}\mathrm{d}\mathbf{p}_i^{(1)}\cdots\mathrm{d}\mathbf{p}_i^{(P)}$$
$$\times\exp\left\{-\beta\sum_{k=1}^{P}\left[\sum_{i=1}^{N}\frac{\mathbf{p}_i^{(k)2}}{2m_i'}+\sum_{i=1}^{N}\frac{1}{2}m_i\omega_P^2\left(\mathbf{r}_i^{(k+1)}-\mathbf{r}_i^{(k)}\right)^2+\frac{1}{2}U\left(\mathbf{r}_1^{(k)},\ldots,\mathbf{r}_N^{(k)}\right)\right]\right\}$$

Eqn. 1. Partition Function of the quantum system. This shows from where the bead spring model originates.

Driven Adiabatic Free Energy Dynamics

- Employs a massive high energy virtual particle which couples to the physical particles → it drags the physical particles around the accessible phase space, allowing for a faster sampling of rare events (points of high free energy)

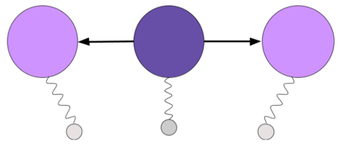

Figure 4. Visualization of driven adiabatic free energy dynamics. The purple ball is the virtual particle and the gray is the physical.

$$F_\alpha(s) = \langle\kappa_\alpha\left(q_\alpha(\mathbf{r})-s_\alpha\right)\rangle$$

Eqn. 3. Mean force of the system.

$$A(s_1,\ldots,s_\alpha) = -\int\prod_{\alpha=1}^{n}F_\alpha(s)\mathrm{d}s_\alpha$$

Eqn. 4. Helmholtz free energy of the system.

$$\tilde{\mathcal{H}}(\mathbf{r},\mathbf{p},s,p) = \mathcal{H}(\mathbf{r},\mathbf{p}) + \sum_{\alpha=1}^{n}\left[\frac{p_\alpha^2}{2\mu_\alpha}+\frac{1}{2}\kappa_\alpha\left(q_\alpha(\mathbf{r})-s_\alpha\right)^2\right]$$

Eqn. 2. Hamiltonian of this system, which describes the total energy and the harmonic coupling of the virtual and physical particle.

Quantum Transition State Theory

- First, calculate the probability of the collective variable hitting the transition state:
- Then, calculate the "static" quantum rate:

$$P(q_c^\ddagger) = \frac{e^{-\beta A(q_c^\ddagger)}}{\int_{q_0^\ddagger}^{q_f^\ddagger}e^{-\beta A(q_c)}\mathrm{d}q_c}$$

Eqn. 5. Probability that the collective variable will pass through the point at the transition state.

$$\ln(k_{\mathrm{QTST}}) = -\frac{\Delta^\ddagger A^\Theta}{R}\cdot\frac{1}{T}+\ln\left(\frac{k_B T}{h}\right)$$

Eqn. 7. Eyring-Polanyi equation. Demonstrates that the log of the rate versus inverse temperature will be roughly linear. The term on top of the R is the activation energy.

$$k_{\mathrm{QTST}} = \frac{1}{\sqrt{2\pi\beta\mu}}P(q_c^\ddagger)$$

Eqn. 6. Static quantum rate constant.

Computational Methodology

$$q_c(\mathbf{r}_c) = \left[\frac{1}{2}\left(\mathbf{r}_c^{H_a}+\mathbf{r}_c^{H_b}\right)-\mathbf{R}_A\right]\cdot\hat{\mu}_{AB}-\frac{|\mathbf{R}_B-\mathbf{R}_A|}{2}$$

Eqn. 8. Collective variable used in this study.

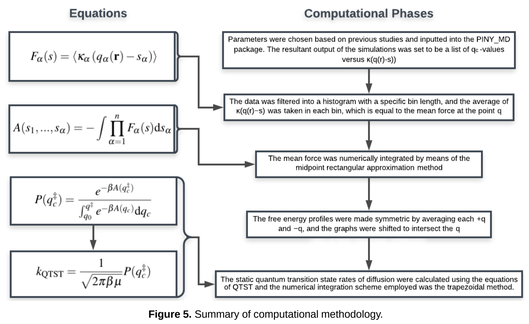

Figure 5. Summary of computational methodology.

RESULTS

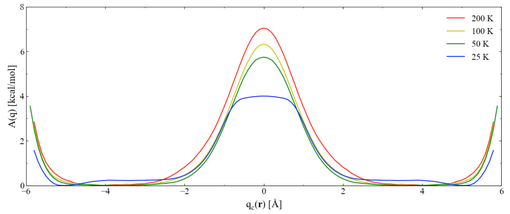

Figure 6. The free energy profile for rigid cage simulations at each of the specified temperature, shifted down for comparison.

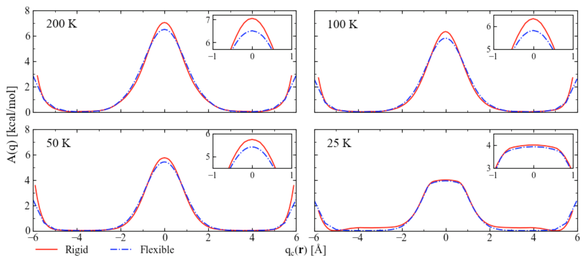

Figure 7. The free energy profile of rigid cage simulations versus flexible cage simulations at each specified temperature. The inset graph in each corner zooms in on the profile near the transition state.

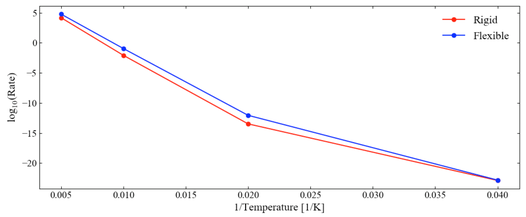

Figure 8. The static quantum rates for both the rigid and flexible cage simulations at 25 K, 50 K, 100 K, and 200 K. The log and inverse scales make the graph linear and thus more view-able.

Temperature	Rigid Rate	Flexible Rate	Factor of Increase
200 K	$1.517\cdot10^{4}$	$5.960\cdot10^{4}$	$3.928\cdot10^{0}$
100 K	$8.343\cdot10^{-3}$	$1.124\cdot10^{-1}$	$1.348\cdot10^{1}$
50 K	$3.327\cdot10^{-14}$	$8.921\cdot10^{-13}$	$2.648\cdot10^{1}$
25 K	$1.319\cdot10^{-23}$	$1.523\cdot10^{-23}$	$1.155\cdot10^{0}$

Table 1. Comparison of the rates from the rigid cage and flexible cage simulations. All rates are in units of [1/s] and all values are rounded to 3 decimal places (the actual values are much more precise).

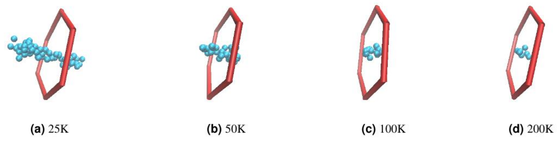

(a) 25K **(b)** 50K **(c)** 100K **(d)** 200K

Figure 9. Visualizations of the beads at the transition state for each temperature (created using VMD).

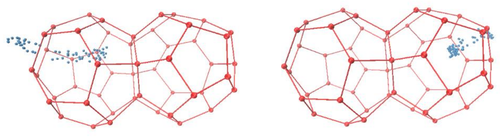

Figure 10. Visualizations of the beads bursting from the sides of the cages (created using VMD).

DISCUSSION

Interpretation of Results

Figure 6

A temperature comparison indicates that, as expected, tunneling is more present at lower temperatures

Also, the dip in the 25 K curve is due to simulation error (discussed later)

Figure 7

Flexibility vs Rigid graphs at each temperature indicate that flexible cages have lower free energies (as hypothesized)

Also, as temperature decreases, the curves get closer together, since flexible cages can't expand at low temperatures even if there is no constraint imposed

Figure 8

Rates graphed on a log scale show that, as expected from the previous graphs, the flexible rates are higher than the rigid rates at each point, and the rates move closer together at the low temperatures

Table 1 + Figure 9

Table 1. and Figure 7. indicate that the mid-range temperatures have larger differences between the rates. This is likely due to the shape of the bead spring necklace

Figure 10

Due to the use of a soft harmonic barrier, some of the beads poked out of the walls, and this ended up causing the dip in the 25 K data. This however, doesn't change the conclusions from the results because the expected results still occurred, and either way, the main temperatures scientists care about are around 100 K anyway.

Discovery

It is without doubt that flexibility of the cages affects the free energy and diffusion rates of hydrogen, so simulations in the future must not assume cage rigidity.

Conclusion

The next steps are either to expand simulation scale or to look further into the effects of cage occupancy. This study is crucial for those next steps so that sufficient accuracy is maintained throughout simulation.

In time, hopefully clathrate hydrate researchers can use these results to put forth an efficient and elegant solution to hydrogen storage, promoting the switch to alternative energy.

REFERENCES

1. Union of Concerned Scientists, "The Hidden Costs of Fossil Fuels," August 30, 2016. [Online]. Available: https://www.ucsusa.org/clean-energy/coal-and-other-fossil-fuels/hidden-cost-of-fossils.
2. Kerschner, C., Prell, C., Feng, K. & Hubacek, K. Economic vulnerability to peak oil. *Glob. Environ. Chang.* **23**, 1424–1433, DOI: https://doi.org/10.1016/j.gloenvcha.2013.08.015 (2013).
3. Brandt, A. R., M.-Ball, A., Ganser, M. & Gorelick, S. M. Peak oil demand: The role of fuel efficiency and alternative fuels in a global oil production decline. *Environ. Sci. Technol.* **47**, 8031–8041, DOI: https://doi.org/10.1021/es401419t (2013).
4. Intergovernmental Panel on Climate Change (IPCC), "Climate Change 2014 Synthesis Report Summary for Policymakers," 2014. [Online]. Available: http://ipcc.ch/pdf/assessment-report/ar5/syr/AR5_SYR_FINAL_SPM.pdf.
5. Epstein, P. R. *et al.* Full cost accounting for the life cycle of coal. *Ann. N.Y. Acad. Sci.* **1219**, 73–98, DOI: https://doi.org/10.1111/j.1749-6632.2010.05890.x (2011).
6. Environmental Protection Agency (EPA), "Air pollution emissions trends data," Washington, DC, 2016. [Online]. Available: https://www.epa.gov/air-emissions-inventories/air-pollutant-emissions-trends-data.
7. Environmental Protection Agency (EPA), "Nitrogen oxides (NOx) control regulations," Washington, DC, 2016. [Online]. Available: http://www.epa.gov/region1/airquality/nox.html.
8. Environmental Protection Agency (EPA), "Acid rain," Washington, DC, 2016. [Online]. Available: http://www.epa.gov/acidrain/.
9. State of Global Air, "Trends in the global health burden from outdoor air pollution." Accessed October 28, 2018. [Online]. Available: https://www.stateofglobalair.org/health/trends.
10. Agency for Toxic Substances and Disease Registry (ATSDR), "Toxicological profile for Plutonium," January 21, 2015. [Online]. Available: https://www.atsdr.cdc.gov/phs/phs.asp?id=64&tid=19.
11. Beckjord, E. S. *et al.* "The Future of Nuclear Power AN INTERDISCIPLINARY MIT STUDY." [Online]. Available: https://web.mit.edu/nuclearpower/pdf/nuclearpower-full.pdf.
12. Taebi, B. The morally desirable option for nuclear power production. *Philos. Technol.* **24**, 169–192, DOI: https://doi.org/10.1007/s13347-011-0022-y (2011).
13. Carley, S., Davies, L. L., Spence, D. B. & Zirogiannis, N. Empirical evaluation of the stringency and design of renewable portfolio standards. *Nat. Energy* **3**, 754–763, DOI: https://doi.org/10.1038/s41560-018-0202-4 (2018).
14. Science Daily, "Managing renewable energy intelligently," March 25, 2014. [Online]. Available: www.sciencedaily.com/releases/2014/03/140325094814.htm.
15. Zheng, W. *et al.* Durable and self-hydrating tungsten carbide-based composite polymer electrolyte membrane fuel cells. *Nat. Commun.* **8**, 418, DOI: https://doi.org/10.1038/s41467-017-00507-6 (2017).
16. Zhu, M. *et al.* Metal-free photocatalyst for h2 evolution in visible to near-infrared region: Black phosphorus/graphitic carbon nitride. *J. Am. Chem. Soc.* **139**, 13234–13242, DOI: https://doi.org/10.1021/jacs.7b08416 (2017).
17. Guo, L. *et al.* MoS$_2$/TiO$_2$ heterostructures as nonmetal plasmonic photocatalysts for highly efficient hydrogen evolution. *Energy Environ. Sci.* **11**, 106–114, DOI: https://doi.org/10.1039/C7EE02464A (2018).
18. Bockris, J. O. Energy, the solar-hydrogen alternative. *Int. J. Energy Res.* **1**, 369–369, DOI: https://doi.org/10.1002/er.4440010409 (1977).
19. Züttel, A. Hydrogen storage methods. *Naturwissenschaften* **91**, 157–172, DOI: https://doi.org/10.1007/s00114-004-0516-x (2004).
20. *Fire Protection Guide to Hazardous Materials, 2010 Edition*, National Fire Protection Association, 2010.
21. Universal Industrial Gases, Inc., *Material Safety Data Sheet Gaseous Hydrogen*, MSDS H2-G, 2015. [Online]. Available: http://www.uigi.com/MSDS_gaseous_H2.html.
22. Environmental Protection Agency (EPA), "Safety and Security Analysis: Investigative Report by NASA on Proposed EPA Hydrogen-Powered Vehicle Fueling Station," Rep. EPA420-R-04-016, 2004. [Online]. Available: https://archive.epa.gov/otaq/fuelcell/web/pdf/420r04016.pdf.
23. Struzhkin, V. V., Militzer, B., Mao, W. L., Mao, H.-K. & Hemley, R. J. Hydrogen storage in molecular clathrates. *Chem. Rev.* **107**, 4133–4151, DOI: https://doi.org/10.1021/cr050183d (2007).
24. Sloan, E. D. & Koh, C. A. *Clathrate Hydrates of Natural Gases* (CRC Press, Taylor and Francis Group, Boca Raton, FL, 2008).
25. Mao, W. L. *et al.* Hydrogen clusters in clathrate hydrate. *Science* **297**, 2247–2249, DOI: https://doi.org/10.1126/science.1075394 (2002).
26. DOE. https://www.energy.gov/eere/fuelcells/doe-technical-targets-onboard-hydrogen-storage-light-duty-vehicles, the targets for future hydrogen storage economy as defined by the Department of Energy.
27. Cendagorta, J. R. *et al.* Competing quantum effects in the free energy profiles and diffusion rates of hydrogen and deuterium molecules through clathrate hydrates. *Phys. Chem. Chem. Phys.* **18**, 32169–32177, DOI: http://dx.doi.org/10.1039/C6CP05906F (2016).
28. Mao, W. L. & Mao, H.-K. Hydrogen storage in molecular compounds. *Proc. Natl. Acad. Sci. USA* **101**, 708–710, DOI: https://doi.org/10.1073/pnas.0307449100 (2004).
29. Vos, W. L., Finger, L. W., Hemley, R. J. & Mao, H.-K. Pressure dependence of hydrogen bonding in a novel $H_2O\cdot H_2$ clathrate. *Chem. Phys. Lett.* **257**, 524–530, DOI: https://doi.org/10.1016/0009-2614(96)00583-0 (1996).
30. Trinh, T. T., Waage, M. H., van Erp, T. S. & Kjelstrup, S. Low barriers for hydrogen diffusion in sii clathrate. *Phys. Chem. Chem. Phys.* **17**, 13808–13812, DOI: https://doi.org/10.1039/C5CP01713K (2015).
31. Alavi, S., Ripmeester, J. A. & Klug, D. D. Molecular-dynamics study of structure ii hydrogen clathrates. *J. Chem. Phys.* **123**, 024507, DOI: https://doi.org/10.1063/1.1953577 (2005).
32. Alavi, S. & Ripmeester, J. A. Hydrogen-gas migration through clathrate hydrate cages. *Angew. Chem.* **46**, 8933–8935, DOI: https://doi.org/10.1002/anie.200703025#1 (2007).
33. Senadheera, L. & Conradi, M. S. Rotation and diffusion of H_2 in hydrogen-ice clathrate by h nmr. *J. Phys. Chem. B* **111**, 12097–12102, DOI: https://doi.org/10.1021/jp074517+ (2007).
34. Ohachi, T., Moudrakovski, I. L. & Ripmeester, J. A. Efficient storage of hydrogen fuel into leaky cages of clathrate hydrate. *Appl. Phys. Lett.* **91**, 171903, DOI: https://doi.org/10.1063/1.2802041 (2007).
35. Yoshioka, H. *et al.* Decomposition kinetics and recycle of binary hydrogen-tetrahydrofuran clathrate hydrate. *AIChE J.* **57**, 265–272, DOI: https://doi.org/10.1002/aic.12241 (2011).
36. Burnham, C. J., Futera, Z. & English, N. J. Quantum and classical inter-cage hopping of hydrogen molecules in clathrate hydrate: temperature and cage-occupation effects. *Phys. Chem. Chem. Phys.* **19**, 717–728, DOI: https://doi.org/10.1039/C6CP06531G (2017).
37. Feynamn, R. P. & Hibbs, A. R. *Quantum Mechanics and Path Integrals* (McGraw-Hill, New York, 1965).
38. Abrams, J. B. & Tuckerman, M. E. Efficient and direct generation of multidimensional free energy surfaces via adiabatic dynamics without coordinate transformations. *J. Phys. Chem. B* **112**, 15742–15757, DOI: https://doi.org/10.1021/jp805039u (2008).
39. Chen, M., Cuendet, M. A. & Tuckerman, M. E. Heating and flooding: A unified approach for rapid generation of free energy surfaces. *J. Chem. Phys.* **137**, 024102, DOI: https://doi.org/10.1063/1.4733389 (2012).
40. Martyna, G. J., Klein, M. L. & Tuckerman, M. E. Nosé–hoover chains: The canonical ensemble via continuous dynamics. *The J. Chem. Phys.* **97**, 2635–2643, DOI: https://doi.org/10.1063/1.463940 (1992).
41. Margul, D. T. & Tuckerman, M. E. A stochastic, resonance-free multiple time-step algorithm for polarizable models that permits very large time steps. *J. Chem. Theory Comput.* **12**, 2170–2180, DOI: https://doi.org/10.1021/acs.jctc.6b00188 (2016).
42. Tuckerman, M. E., Yarne, D. A., Samuelson, S. O., Hughes, A. L. & Martyna, G. J. Exploiting multiple levels of parallelism in molecular dynamics based calculations via modern techniques and software paradigms on distributed memory computers. *Comput. Phys. Commun.* **128**, 333 – 376, DOI: https://doi.org/10.1016/S0010-4655(00)00077-1 (2000).